Article

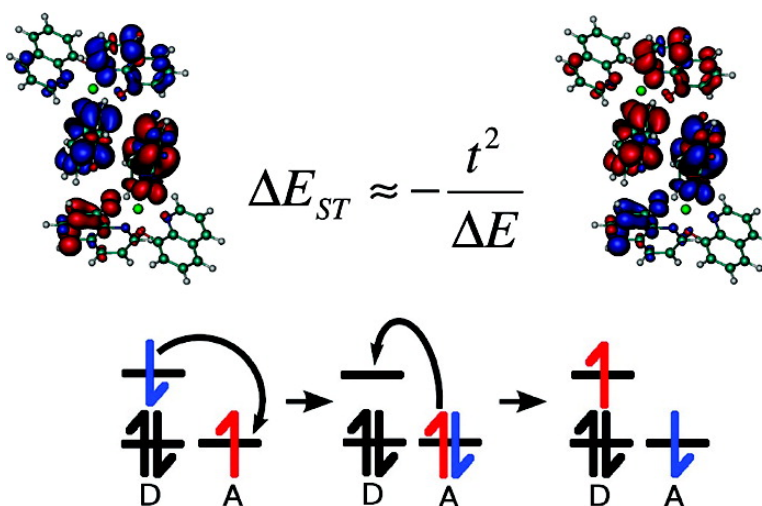# On the Singlet–Triplet Splitting of Geminate Electron–Hole Pairs in Organic Semiconductors

Seth Difley, David Beljonne, and Troy Van Voorhis

$$\Delta E_{ST} \approx -\frac{t^2}{\Delta E}$$

More About This Article

Additional resources and features associated with this article are available within the HTML version:

- Supporting Information
- Links to the 1 articles that cite this article, as of the time of this article download
- Access to high resolution figures
- Links to articles and content related to this article
- Copyright permission to reproduce figures and/or text from this article

View the Full Text HTML

On the Singlet−Triplet Splitting of Geminate Electron−Hole Pairs in Organic Semiconductors

Seth Difley,[†] David Beljonne,[‡] and Troy Van Voorhis*,[†]

Department of Chemistry, Massachusetts Institute of Technology, 77 Massachusetts Avenue, Cambridge, Massachusetts 02139, and Laboratory for Chemistry of Novel Materials, Université de Mons-Hainaut, Place du Parc, 20, 7000 Mons, Belgium

Received August 14, 2007; E-mail: tvan@mit.edu

Abstract: Because of their unique photophysical properties, organic semiconductors have shown great promise in both light-emitting devices (LEDs) and photovoltaic systems. In particular, the question of *spin statistics* looms large in these applications: the relative energetics and rates of formation for singlet versus triplet excited states can have a significant impact on device efficiency. In this Article, we study the singlet and triplet charge-transfer (CT) configurations that can be thought of as the immediate precursors to the luminescent states in organic LEDs. In particular, we find that the CT singlet−triplet energy gap (ΔE_{ST}) of organic dyes and oligomers depends sensitively on both the material and the relative orientation of the donor/acceptor pair. Furthermore, in contrast with the commonly held view, we find that the singlet CT states nearly always lie energetically below the triplet CT states ($\Delta E_{ST} < 0$). This trend is attributed to two physical sources. First, the relatively close contact between the donor and acceptor leads to a strong kinetic exchange component that favors the singlet. Second, Coulombic attraction between the separated charges favors inner-sphere reorganization that brings the donor and acceptor closer together, further enhancing the kinetic exchange effect. We discuss the implications of these results on the design of organic LEDs.

1. Introduction

Due to their unusual mechanical and photophysical properties, organic semiconductors show promise in the development of a variety of innovative technologies: inexpensive light-emitting devices (LEDs),[1] flexible transistors,[2] and novel photovoltaic architectures,[3] just to name a few. Typically, these organic materials involve weakly bound assemblies of π-conjugated molecules or polymers whose electro-optical properties rest on a complex interplay between electron-transfer kinetics,[4] organic photochemistry,[5] and organic/inorganic interfacial structure.[6] In the search for improved performance, chemistry plays a central role by providing information about the participating states, including their formation rates, lifetimes, and decay pathways, ultimately facilitating the rational design of novel devices.

Of special interest in this context are the charge-transfer (CT) states that determine both the transport properties of the material and the exciton dissociation/recombination rates that govern electroluminescent and photovoltaic efficiency.[7] In particular, CT excited states play a crucial role in the operation of organic light-emitting devices (OLEDs).[8−11] OLED-based display tech-

nologies are a promising alternative to traditional inorganic LED-based displays because they can be brighter, more adaptable, longer-lived, and more energy efficient. Basic OLEDs consist of a solid-state emitting layer (EML) containing electron- and hole-accepting molecules sandwiched between an anode and a cathode.[12] Electrons (holes) injected at the cathode (anode) enter the EML and diffuse through it, eventually migrating onto adjacent molecules to form a CT state, which is an intermolecular charge-separated donor−acceptor pair (D^+A^-). Once the CT state has formed, it is bound by the Coulombic force that results from the charge separation. Because the electron and hole are both spin $^1/_2$, the CT state will be either a singlet or a triplet. Sometime after CT state formation, the electron and hole may undergo charge recombination to form an exciton that will typically have the same spin symmetry as the CT state. Singlet excitons can undergo efficient fluorescent decay to the ground state, while triplet excitons decay to the singlet ground state by phosphorescence, an inefficient process in the absence of spin−orbit coupling.[13] Thus, the question of spin statistics—what fraction of excitons are created as singlets as compared to triplets—plays a key role in OLED efficiency.

Assuming that the CT states are formed from electrons and holes having a random distribution of spin symmetry, three triplet CT states will be formed for each singlet CT state. If

† Massachusetts Institute of Technology.
‡ Université de Mons-Hainaut.
(1) Friend, R. H.; Gymer, R. W.; Holmes, A. B.; Burroughes, J. H.; Marks, R. N.; Taliani, C.; Bradley, D. D. C.; Santos, D. A. D.; Brédas, J. L.; Logdlund, M.; Salaneck, W. R. *Nature* **1999**, *397*, 121−128.
(2) Horowitz, G. *Adv. Mater.* **1998**, *10*, 365−377.
(3) Nozik, A. J. *Annu. Rev. Phys. Chem.* **1978**, *29*, 189−222.
(4) Coropceanu, V.; Cornil, J.; da Silva, Fiho, D. A.; Olivier, Y.; Silbey, R.; Brédas, J. L. *Chem. Rev.* **2007**, *107*, 926−952.
(5) Mitschke, U.; Bauerle, P. *J. Mater. Chem.* **2000**, *10*, 1471.
(6) Judenstein, P.; Sanchez, C. *J. Mater. Chem.* **1996**, *6*, 511−525.
(7) Brédas, J.-L.; Beljonne, D.; Coropceanu, V.; Cornil, J. *Chem. Rev.* **2004**, *104*, 4971−5003.

(8) Sheats, J. R.; Antoniadis, H.; Hueschen, M.; Leonard, W.; Miller, J.; Moon, R.; Roitman, D.; Stocking, A. *Science* **1996**, *273*, 884−888.
(9) Forrest, S. R. *Nature* **2004**, *428*, 911−918.
(10) Geffroy, B.; le Roy, P.; Prat, C. *Polym. Int.* **2006**, *55*, 572−582.
(11) Shen, Z.; Burrows, P. E.; Bulović, V.; Forrest, S. R.; Thompson, M. E. *Science* **1997**, *276*, 2009−2011.
(12) Helfrich, W.; Schneider, W. G. *Phys. Rev. Lett.* **1965**, *14*, 229−231.
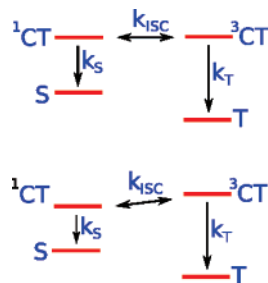(13) Yersin, H. *Top. Curr. Chem.* **2004**, *241*, 1−26.

Figure 1. Exciton formation pathways assuming nearly degenerate CT states (top) and $\Delta E_{ST} < 0$ (bottom). Singlet and triplet excitons are, respectively, labeled S and T.

intersystem crossing (ISC), which interchanges singlet and triplet CT states, is negligible, the fraction of singlet excitons formed will be one-quarter and the expected fluorescent efficiency will be 25%. The literature does contain numerous reports where this simple statistical limit is actually observed,[14,15] but there are also multiple reports of >25% fluorescent efficiency[16−22] and a variety of theoretical work has been conducted on OLED exciton formation[23−33] to address these observations.

The conventional picture of enhanced fluorescence that emerges from this work, first postulated in ref 23 (see Figure 1), focuses on the rate of triplet exciton formation, k_T. One notes that the driving force for triplet charge recombination, $\Delta G_T \equiv E_{CT_T} − E_T$, for an organic dye or oligomer is typically 0.5−0.7 eV greater than its singlet counterpart, $\Delta G_S \equiv E_{CT_S} − E_S$.[34,35] Furthermore, electron transfer for these materials typically occurs in the Marcus inverted region because the energy gaps involved are many times the associated reorganization energies. Thus, the recombination rate is expected to *decrease* as the energy gap *increases*. From these observations, the conventional view predicts that triplet exciton formation will be much slower

than the analogous singlet rate, $k_T \ll k_S$, because $\Delta G_T \gg \Delta G_S$. As a result, one could potentially obtain efficiencies that exceed 25% if the ISC rate, k_{ISC}, is competitive with the rate of triplet exciton formation, k_T, but much less than the corresponding singlet rate, k_S. That is, fluorescence is enhanced if $k_S \gg k_{ISC} \geq k_T$. On the other hand, if k_T is faster than k_{ISC} (though it may still be slower than k_S) an efficiency of 25% could be observed. One problematic point of this interpretation is that it leads one to assume that high-efficiency fluorescence should occur when ΔG_T is large and that statistically expected 25% efficiency will occur for small ΔG_T values. However, this correlation has not been observed in practice. To explain this, it has been proposed that in cases where the statistical limit is observed, dark triplet states between the triplet exciton and ground state can make k_T much faster than it otherwise would be,[7] thereby exceeding the intersystem crossing rate and leading to the formation of a 1:3 ratio of singlet-to-triplet excitons.

In this paper, we examine an alternative hypothesis for the variation of singlet formation efficiencies, which focuses on the variation of k_{ISC} between different organic semiconducting materials. In particular, while there are many processes which will influence this rate in real systems (e.g., spin−orbit coupling, spin−lattice relaxation, hyperfine interactions, etc.) which are quite difficult to compute, there is one factor which can be simulated—the singlet−triplet CT energy gap (ΔE_{ST}). In particular, one expects that, as suggested previously,[36] if ΔE_{ST} is sufficiently large, k_{ISC} (Figure 1, bottom) will be very slow relative to both k_S and k_T and the resulting singlet−triplet exciton formation ratio will be 1:3. Meanwhile for small ΔE_{ST} values, the fluorescence efficiency could still exceed 25% in the standard way (Figure 1, top). Thus, in this view, the material and geometry dependence of ΔE_{ST} can play a crucial role in determining the fluorescence efficiency of a given device. To examine the validity of this picture, we use simulations to estimate the singlet−triplet CT state splitting, ΔE_{ST}, in dimers of several low-to-medium weight chromophores and oligomers and discover several surprising results. First, ΔE_{ST} is strongly material-dependent, changing magnitude and even sign depending on the system being studied. Second, in contrast with the commonly held view, we find that the singlet CT state nearly always lies below the triplet CT state ($\Delta E_{ST} < 0$). This result is explained in terms of two related physical properties. First, at the short intermolecular distances present in CT states, the exchange interaction is dominated by kinetic exchange, which favors the singlet state. Second, Coulombic interaction within the CT state causes reorganization that decreases the distance between the electron and hole and further increases the singlet-favoring kinetic exchange. Implications of these results on the design of efficient OLEDs are discussed. In particular, our finding that ΔE_{ST} is generally nonzero suggests that OLEDs typically will experience slow intersystem crossing and, therefore, low fluorescence efficiency if spin−orbit coupling is absent. However, as recently shown,[37] the insertion of a sensitizer that mixes the CT states while leaving the exciton states unmixed leads to a much more efficient OLED.

(14) Segal, M.; Baldo, M. A.; Holmes, R. J.; Forrest, S. R.; Soos, Z. G. *Phys. Rev. B: Condens. Matter Mater. Phys.* **2003**, *68*, 075211.
(15) Lin, L. C.; Meng, H. F.; Shy, J. T.; Horng, S. F.; Yu, L. S.; Chen, C. H.; Liaw, H. H.; Huang, C. C.; Peng, K. Y.; Chen, S. A. *Phys. Rev. Lett.* **2003**, *90*, 036601.
(16) Cao, Y.; Parker, I. D.; Yu, G.; Zhang, C.; Heeger, A. J. *Nature* **1998**, *397*, 414−417.
(17) Ho, P. K. H.; Kim, J.-S.; Burroughes, J. H.; Becker, H.; Li, S. F. Y.; Brown, T. M.; Cacialli, F.; Friend, R. H. *Nature* **2000**, *404*, 481−484.
(18) Wilson, J. S.; Dhoot, A. S.; Seeley, A. J. A. B.; Khan, M. S.; Köhl, A.; Friend, R. H. *Nature* **2001**, *413*, 828−831.
(19) Wohlgenannt, M.; Tandon, K.; Mazumdar, S.; Ramasesha, S.; Vardeny, Z. V. *Nature* **2001**, *409*, 494−497.
(20) Wohlgenannt, M.; Jiang, X. M.; Vardeny, Z. V.; Janssen, R. A. J. *Phys. Rev. Lett.* **2002**, *88*, 197401.
(21) Wohlgenannt, M.; Yang, C.; Vardeny, Z. V. *Phys. Rev. B: Condens. Matter Mater. Phys.* **2002**, *66*, 241201.
(22) Dhoot, A. S.; Ginger, D. S.; Beljonne, D.; Shuai, Z.; Greenham, N. C. *Chem. Phys. Lett.* **2002**, *360*, 195−201.
(23) Shuai, Z.; Beljonne, D.; Silbey, R. J.; Brédas, J. L. *Phys. Rev. Lett.* **2000**, *84*, 131−134.
(24) Wohlgenannt, M. *Phys. Status Solidi A* **2004**, *201*, 1188−1204.
(25) Wohlgenannt, M.; Vardeny, Z. V. *J. Phys.: Condens. Matter* **2003**, *15*, R83−R107.
(26) Barford, W. *Phys. Rev. B: Condens. Matter Mater. Phys.* **2004**, *70*, 205204.
(27) Kobrak, M. N.; Bittner, E. R. *Phys. Rev. B: Condens. Matter Mater. Phys.* **2000**, *62*, 11473.
(28) Staudigel, J.; Stössel, M.; Steuber, F.; Simmerer, J. *J. Appl. Phys.* **1999**, *86*, 3895−3910.
(29) Burin, A. L.; Ratner, M. A. *J. Chem. Phys.* **1998**, *109*, 6092−6102.
(30) Karabunarliev, S.; Bittner, E. R. *J. Chem. Phys.* **2003**, *119*, 3988−3995.
(31) Hong, T.-M.; Meng, H.-F. *Phys. Rev. B: Condens. Matter Mater. Phys.* **2001**, *63*, 075206.
(32) Ye, Z.; Shuai, Z.; Brédas, J. L. *Phys. Rev. B: Condens. Matter Mater. Phys.* **2002**, *65*, 045208.
(33) Tandon, K.; Ramasesha, S.; Mazumdar, S. *Phys. Rev. B: Condens. Matter Mater. Phys.* **2003**, *67*, 045109.
(34) Köhle, A.; Wilson, J. S.; Friend, R. H.; Al-Suti, M. K.; Khan, M. S.; Gerhard, A.; Bässler, H. *J. Chem. Phys.* **2002**, *116*, 9457−9463.
(35) Rothe, C.; Brunner, K.; Bach, I.; Heun, S.; Monkman, A. P. *J. Chem. Phys.* **2005**, *122*, 084706.
(36) Reufer, M.; Walter, M. J.; Lagoudakis, P. G.; Hummel, A. B.; Kolb, J. S.; Roskos, H. G.; Scherf, U.; Lupton, J. M. *Nat. Mater.* **2005**, *4*, 340−346.
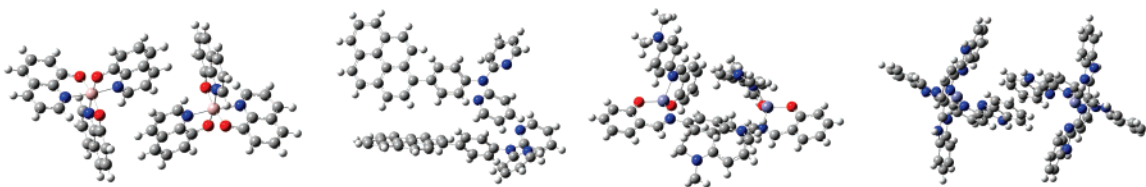(37) Segal, M.; Singh, M.; Rivoire, K.; Difley, S.; Voorhis, T. V.; Baldo, M. A. *Nat. Mater.* **2007**, *6*, 374−378.

Figure 2. Representative dimer structures from Table 2. From left to right: α-Alq$_3$, 4-(1-pyrenyl)phenyl-2,2′-dipyridylamine, Zn(sada)$_2$, and [Zn(tpy)$_2$]$^{2+}$.

2. Methods

2.1. Constrained Density Functional Theory (C-DFT). We use C-DFT to compute the singlet−triplet gaps in CT states. The details of this approach, which uses constraints to compute both charge-transfer excited states and exchange couplings, have been detailed elsewhere.[38,39] Here, we briefly review C-DFT and illustrate the use of this computational tool.

In the C-DFT formalism, we build constraints of the form

$$\sum_{\sigma} \int w_c^{\sigma}(\mathbf{r})\rho^{\sigma}(\mathbf{r}) \, d\mathbf{r} = N_c \qquad (1)$$

where the sum is over spins such that $\sigma = \uparrow$ or $\downarrow$, c is the constrained region of the system, w_c is a weighting function that corresponds to the constrained property, and N_c is the expectation value of the constrained property. Equation 1 is then combined as a Lagrange multiplier constraint with the Kohn−Sham energy functional $E[\rho]$ to generate a new functional

$$W[\rho, \{V_c\}] = E[\rho] + \sum_{c}^{m} V_c \left(\sum_{\sigma} \int w_c^{\sigma}(\mathbf{r})\rho^{\sigma}(\mathbf{r}) \, d\mathbf{r} - N_c \right) \quad (2)$$

where the cth Lagrange multiplier is V_c and there are m constraints. W is then made stationary with respect to ρ and V_c. By this procedure, we obtain the energy $E(\rho)$ as a natural function of the expectation value N_c. The utility of this method has been previously demonstrated for studying magnetic exchange couplings using spin constraints[39] and to obtain Marcus parameters[40,41] and study long-range electron transfer[42] using charge constraints.

In the present study of CT state singlet−triplet splittings, both charge and spin constraints are used. These calculations are performed on a supersystem containing a donor and an acceptor molecule. Two separate constrained calculations are performed on the donor−acceptor system, one in which the excess spins are parallel ($\uparrow\uparrow$) and one in which they are antiparallel ($\uparrow\downarrow$). Note that the $\uparrow\downarrow$ configuration will be referred to as the "mixed" state because it is a mixture of $M_S = 0$ singlet and $M_S = 0$ triplet spin states. The $\uparrow\uparrow$ configuration will be referred to as the triplet state. A charge constraint is applied that forces the acceptor to have an excess charge of −1. A concurrent constraint on the net spin forces the donor and acceptor, respectively, to have excess spin of $\pm^1/_2$. Since the spin component of the singlet state is $1/\sqrt{2}$ ($|\uparrow\downarrow\rangle - |\downarrow\uparrow\rangle$), the singlet−triplet gap ΔE_{ST} is twice the energy difference between the parallel and antiparallel states.[43]

$$\Delta E_{ST} = 2(E_{\uparrow\downarrow} - E_{\uparrow\uparrow}) \qquad (3)$$

These calculations neglect the effects of neighboring molecules on the active dimer. That is, crystal packing constraints and outer-sphere reorganization are absent from our model. However, our models do consider the contribution of the inner-sphere reorganization to the CT state splitting in these systems.

2.2. Computational Details. Constrained calculations were performed using versions of *NWChem*[44] and *QChem*[45] in which C-DFT has been implemented. All calculations described herein were computed using the B3LYP hybrid functional. Meanwhile, the LANL2DZ effective core potential was employed when necessary. The 3-21G basis set was used unless otherwise indicated. When dimer crystal structures were available, these were taken to be the neutral-state geometries. In cases where crystal structure geometries were unavailable, a geometry guess was constructed by placing the donor and acceptor at a reasonable long-range distance of about 3.5 Å and oriented such that the ground-state highest occupied molecular orbital (HOMO) orbital on the acceptor was in the proximity of the ground-state lowest unoccupied molecular orbital (LUMO) on the donor. CT state geometries were obtained by optimizing this initial geometry subject to the corresponding population constraints. The geometries used in these calculations are available in the Supporting Information. The weighting function $w_c(\mathbf{r})$ in eq 2, which measures the net charge and spin, may be reasonably defined in several ways. The calculations presented here use the definition of Becke.[46]

In this Article, we study the CT system in the moment immediately before charge recombination and the geometry of the system in this configuration can have a significant influence on the energetics. When the system is promoted from neutral to CT, relaxation toward the CT state's optimal geometry will naturally occur. If the charge-transfer process is fast relative to this reorganization, the relevant charge recombination geometry will be near the initial, neutral-state geometry. On the other hand, if the charge-transfer process is slow relative to reorganization, the relevant geometry is expected to be nearer to the CT state optimal geometry. Since the relative rates of these processes are not known, it is useful to compute splittings in both limits.

3. Results

To grossly characterize the behavior of ΔE_{ST} for organic chromophores, we computed the splitting for a series of homonuclear dimers formed from low-molecular-weight dyes. For reference, representative structures of these dimers are shown in Figure 2. Alq$_3$ was chosen because it is the prototypical material used as the emitting layer in many model OLEDs.[37] Here, there are three different polymorphs of the crystal with slightly different photophysical properties. In particular, the δ phase consists of the fac isomer of Alq$_3$, as opposed to the mer isomer present in the α and β phases. The change in monomer structure and reduced π interaction in the excited state gives rise to a blue-shift in the spectrum, making δ-Alq$_3$ a blue emitter.[47,48] The dipyridylamine (dpa) complexes were chosen because of their unusual ability to emit in the deep blue.[49] Zn-

(38) Wu, Q.; Voorhis, T. V. *Phys. Rev. A: At., Mol., Opt. Phys.* **2005**, *72*, 024502.
(39) Rudra, I.; Wu, Q.; Voorhis, T. V. *J. Chem. Phys.* **2006**, *124*, 24103.
(40) Wu, Q.; Voorhis, T. V. *J. Phys. Chem. A* **2006**, *110*, 9212−9218.
(41) Wu, Q.; Voorhis, T. V. *J. Chem. Phys.* **2006**, *125*, 164105.
(42) Wu, Q.; Voorhis, T. V. *J. Chem. Theory Comput.* **2006**, *2*, 765−774.
(43) Ziegler, T.; Rauk, A.; Baerends, E. J. *Theoret. Chim. Acta* **1977**, *43*, 261−271.

(44) High Performance Computational Chemistry Group. *NWChem, A Computational Chemistry Package for Parallel Computers,* version 4.6; Pacific Northwest National Laboratory: Richland, WA, 2004.
(45) Kong, J. et al. *J. Comput. Chem.* **2000**, *21*, 1532−1548.
(46) Becke, A. D. *J. Chem. Phys.* **1988**, *88*, 2547.
(47) Cölle, M.; Dinnebier, R. E.; Brütting, W. *Chem. Commun.* **2002**, *23*, 2908−2909.
(48) Braun, M.; Gmeiner, J.; Tzolov, M.; Coelle, M.; Meyer, F. D.; Milius, W.; Hillebrecht, H.; Wendland, O.; von Schtz, J. U.; Brtting, W. *J. Chem. Phys.* **2001**, *114*, 9625−9632.

Table 1. Calculated and Experimental Singlet (S) and Triplet (T) Exciton Energies for the Chromophores in Table 2. TDDFT Calculations Were Performed with B3LYP in the 3-21G Basis Set (6-31G* Results Are Shown in Parentheses)

chromophore	TDDFT (eV)		Δ_{SCF} (eV)	exp (eV)	
	S	T	T	S	T
α-Alq$_3$	2.7 (2.7)	2.2 (2.2)	2.4 (2.4)	2.9[a]	2.1[b]
δ-Alq$_3$	2.8 (2.9)	2.2 (2.2)	2.3 (2.3)	2.9[c]	2.2[b]
1-R$_1$-dpa	3.5 (3.4)	2.5 (2.4)	2.5 (2.5)	3.6[d]	
4-R$_2$-dpa	3.4 (3.4)	2.4 (2.3)	2.5 (2.4)	3.6[d]	
4-R$_3$-dpa	3.0 (3.0)	2.4 (2.4)	2.5 (2.4)	3.6[d]	
Zn(sada)$_2$	2.9 (2.9)	2.3 (2.3)	2.4 (2.4)	2.6[e]	
[Zn(bbp)$_2$]$^{2+}$	3.5 (3.3)	2.9 (2.8)	3.1 (3.0)		
[Zn(tpt)$_2$]$^{2+}$	2.4 (2.7)	2.2 (2.6)	2.9 (3.1)		
[Zn(tpy)$_2$]$^{2+}$	3.4 (4.1)	3.2 (3.3)	3.7 (3.4)		

[a] Absorption onset in crystal.[52] [b] Phosphorescence in crystal.[53] [c] Absorption onset in crystal.[47,48] [d] Absorption maximum in THF.[49] [e] Absorption onset in thin film.[50]

Table 2. ΔE_{ST} for Dimers of Several Low-Molecular-Weight Chromophores Computed Using 3-21G and 6-31G* Basis Sets. Metal–Metal Bond Distances and Differences between ↑↓ and Triplet Dipole Magnitudes Are Also Presented

chromophore	ΔE_{ST} (meV)		metal–metal distance (Å)	$\mu_{\uparrow\downarrow} - \mu_{\uparrow\uparrow}$ (debye)
	3-21G	6-31G*		
α-Alq$_3$[a]	−2	−2	8.86	0.07
β-Alq$_3$[a]	−6	−7	11.28	0.00
δ-Alq$_3$[b]	−60	−74	8.87	0.11
1-R$_1$-dpa[c]	−58	−61		0.02
4-R$_2$-dpa[c]	−1	−5		0.00
4-R$_3$-dpa[c]	−30	−42		0.00
Zn(sada)$_2$[d]	−102	−102	8.97	−0.10
[Zn(bbp)$_2$]$^{2+}$[e]	−67	−57	8.67	0.04
[Zn(tpt)$_2$]$^{2+}$[e]	−19	−48	8.95	−0.03
[Zn(tpy)$_2$]$^{2+}$[e]	−85	−89	8.79	−0.23

[a] Alq$_3$ = tris(8-hydroxyquinoline)aluminum(III).[52] [b] Alq$_3$ = tris(8-hydroxyquinoline)aluminum(III).[47] [c] dpa = 2,2′-dipyridylamine, R$_1$ = pyrenyl, R$_2$ = (1-pyrenyl)phenyl, R$_3$ = 4′-(1-pyrenyl)biphenyl.[49] [d] Zn(sada)$_2$ = bis[salicylidene(4-dimethylamino)aniline]zinc(II).[50] [e] bbp = 2,6-bis(1H-benzimidazol-2-yl)pyridine, tpt = 2,4,6-tris(2-pyridyl)-1,3,5-triazine, tpy = 2,20′:6′,2″-terpyridine.[51]

(sada)$_2$ thin films show more common yellow emission with improved charge-transport characteristics.[50] The final three zinc complexes demonstrate the interesting behavior that the crystal packing has a significant influence on the monomer geometry (i.e., the molecule is more flexible) which could lead to interesting effects.[51] Thus, these crystals allow us to test the degree to which different bonding motifs and photophysical properties influence or at least correlate with ΔE_{ST}.

For reference, calculated and experimental singlet and triplet exciton energies for these materials are presented in Table 1. The time-dependent (TDDFT) calculations are vertical excitation energies obtained for isolated monomers taken from the crystal structure. As a result, the theoretical predictions neglect a number of features (e.g., crystal field effects, exciton delocalization, etc.) that are known to be necessary for the accurate prediction of solid-state excitation spectra. Furthermore, we note that not all the experimental numbers are precisely comparable to one another; in some cases the experiments were done in crystals, others were done in thin films, and still others were done in solution. Taking all these points into consideration, one should really consider the calculated numbers and experiments as ballpark estimates of the energies involved here. In this context, TDDFT does a fairly good job of predicting the exciton energies in these materials, typically predicting the exciton energies to within 0.2–0.3 eV.

Next, we turn our attention to the intermolecular CT excited states of these materials. Here we employ constrained DFT, as described in the previous section. Each calculation was performed on a dimer formed from near-neighbor monomers oriented according to the crystal structure. Splittings were obtained for both the 3-21G and 6-31G* basis sets, and the results are compiled in Table 2. Noting that a negative ΔE_{ST} value means that the singlet CT state lies below the triplet CT state, we observe that singlet CT states are stabilized relative to triplet CT states for all of these systems in their crystal structure geometries. This observation contrasts with the general assumption that triplet CT states lie lowest.[34,35,54] Furthermore,

we find that splittings predicted in the two basis sets are similar in both sign and magnitude. While this could potentially be due to a cancellation of errors between the two basis sets, the consistency of the agreement strongly suggests instead that Δ_{ST} is insensitive to basis set, so our results can be considered nearly converged with respect to basis set size. Importantly, the resulting magnitude of ΔE_{ST} implies that intersystem crossing (Figure 1) should be much slower than one would expect from nearly degenerate spin pairs.

While the sign of the splitting is constant across the cases, we find that the magnitude can change significantly from system to system. Furthermore, on the basis of these data alone, it is very difficult to provide case-by-case explanations for why some materials have large splittings and others do not. The variations of ΔE_{ST} *within* a given structural motif are at least as large as the variations *between* different motifs. For example, comparing the three Alq$_3$ phases in Table 2, we observe that modification of the orientation of the monomers can result in differences in the singlet–triplet CT gap by more than an order of magnitude. Perhaps surprisingly, the exchange splitting does not correlate with the intermonomer distance, as evidenced by examining the metal–metal distances shown in Table 2. Rather, it appears that the relative orientation of donor and acceptor plays a more significant role. All of these observations lead to the conclusion that ΔE_{ST} shows strong nontrivial material dependence. The one exception to this may be Zn(sada)$_2$. This material has the largest splitting of any of the compounds and also has the best transport properties. On the basis of the kinetic exchange mechanism we propose below, we expect that this is not a coincidence— materials with high mobilites may tend to have large ΔE_{ST} values as well, as both properties tend to result from good donor–acceptor overlap. Finally, we note the interesting fact that α- and β-Alq$_3$ have nearly degenerate CT states, implying that intersystem crossing could be favorable for these systems (see Figure 1), while for the δ-Alq$_3$ phase, intersystem crossing should be quite strongly hindered.

Overall, the inclusion of the variation of other components of k_{ISC} (e.g., spin–orbit or hyperfine coupling constants) would typically increase the material dependence of these rates. Thus,

(49) Jia, W.-L.; McCormick, T.; Liu, Q.-D.; Fukutani, H.; Motala, M.; Wang, R.-Y.; Tao, Y.; Wang, S. *J. Mater. Chem.* **2004**, *14*, 3344–3350.
(50) Junfeng, X.; Qiao, J.; Wang, L.; Xie, J.; Qiu, Y. *Inorg. Chim. Acta* **2005**, *358*, 4451–4458.
(51) Harvey, M. A.; Baggio, S.; Ibañez, A.; Baggio, R. *Acta. Crystallogr.* **2004**, *C60*, m375–m381.
(52) Brinkmann, M.; Gadret, G.; Muccini, M.; Taliani, C.; Masciocchi, N.; Sironi, A. *J. Am. Chem. Soc.* **2000**, *122*, 5147–5157.
(53) Cölle, M.; Gärditz, C. *J. Lumin.* **2004**, *110*, 200–206.
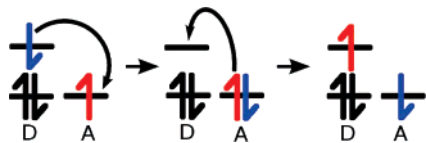(54) Cölle, M.; Gärditz, C. *Appl. Phys. Lett.* **2004**, *84*, 3160–3162.

Figure 3. Kinetic exchange mechanism showing electron exchange between the donor (D) monomer's LUMO and acceptor (A) monomer's HOMO.

one expects that the conclusion of strong material dependence of k_{ISC} will not change qualitatively if more sophisticated treatments of spin relaxation are employed.

To explain how singlet CT states can lie below triplet CT states, we invoke the physical picture of kinetic exchange. Kinetic exchange is a two-step mechanism that swaps the unpaired electrons in the CT state (Figure 3) and has a spin-paired intermediate state. In contrast, direct exchange swaps the electrons in a single step without pairing them. Using perturbation theory and ignoring weaker contributions such as super-exchange, it has been shown[55] that the singlet−triplet splitting should be given by

$$\Delta E_{ST} = -\frac{t^2}{\Delta E} + K \tag{4}$$

where the first and second terms are, respectively, due to kinetic and direct exchange. Here, t is a hopping term between the donor and acceptor, ΔE is an energy difference between the initial and virtual states in the system, and K is a positive exchange integral. The negative sign of the kinetic exchange term corresponds to stabilization of the singlet state relative to the triplet. This stabilization can be thought of as a result of the singlet unpaired electrons lowering their energy by occasionally visiting the same region of space to form the paired intermediate shown in Figure 3. Meanwhile, the triplet unpaired electrons cannot visit the same region of space due to the Pauli exclusion principle and therefore cannot undergo a similar stabilization.

To make use of eq 4, we approximate the hopping term, t, by the overlap, S, between an orbital on the donor and an orbital on the acceptor and assume that ΔE and K do not vary strongly with geometry. Then the variations in ΔE_{ST} will be approximately proportional to S^2 for systems that are dominated by kinetic exchange. Discrepancies from proportionality may be attributed to contributions from other exchange mechanisms[55−57] such as direct, indirect, and superexchange or to a nonconstant value of ΔE. Using this expectation of proportionality, kinetic exchange contributions were examined for homonuclear CT state dimers of two molecules, poly-*p*-phenylene oligomer,[58] intended to mimic a high molecular weight polymer, and DCM (4-dicyanomethylene-2-methyl-6-*p*-dimethylami-nostyryl-4H-pyran),[59] a low-molecular-weight dye. Dimers of each molecule were generated by combining ground-state geometry-optimized monomers in head-to-tail orientation. The planar distances between monomers in the DCM and phenylene dimers, respectively, were 3.50 and 3.65 Å, which represent reasonable monomer separations for near-neighbor CT states. The monomers of each dimer were given initial relative
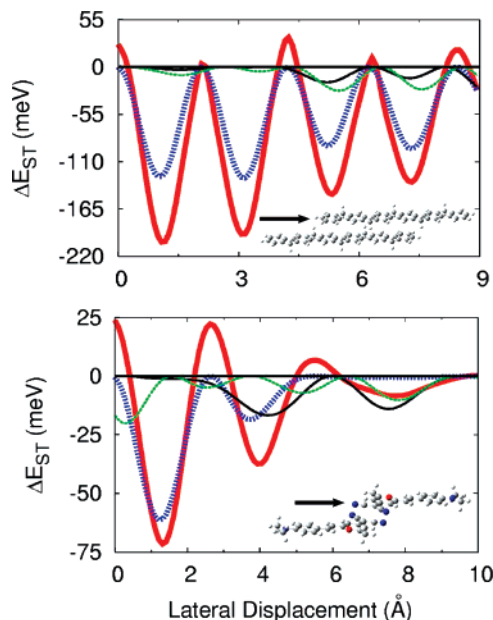
(55) Anderson, P. W. *Phys. Rev.* **1959**, *115*, 2.
(56) Goodenough, J. B. *Phys. Rev.* **1960**, *117*, 1442−1451.
(57) Kanamori, J. *J. Phys. Chem. Solids* **1958**, *10*, 87.
(58) Rissler, J.; Bässler, H. *Phys. Rev. B: Condens. Matter Mater. Phys.* **2001**, *64*, 45122.
(59) Gustavsson, T.; Baldacchino, G.; Mialocq, J.-C.; Pommeret, S. *Chem. Phys. Lett.* **1995**, *236*, 587−594.

Figure 4. ΔE_{ST} (thick solid red curve) and squared orbital overlaps for poly-*p*-phenylene (top) and DCM (bottom) as a function of lateral monomer displacement. Squared overlaps shown in arbitrary units: HOMO/LUMO (thick dashed blue), HOMO−1/LUMO (thin solid black), and HOMO/LUMO+1 (thin dashed green).

orientations and incrementally displaced laterally relative to each other. For each step of this lateral displacement, splittings and donor−acceptor orbital overlaps were computed. (Figure 4). These orbital overlaps were obtained by performing single-point ground-state calculations on each monomer separately to yield molecular orbitals ϕ_D and ϕ_A, respectively, for the isolated donor and acceptor monomers. These unrelaxed orbitals were then rigidly shifted relative to one another to obtain the overlaps at various relative displacements.

For both DCM and poly-*p*-phenylene, Figure 4 shows that ΔE_{ST} and the HOMO/LUMO squared overlap are nearly proportional, indicating that kinetic exchange is the dominant exchange mechanism in these CT state systems. Meanwhile, there is no obvious relationship between ΔE_{ST} and the other orbital overlaps examined in Figure 4, suggesting that interaction between the HOMO and LUMO has a key role in kinetic exchange. Finally, since kinetic exchange only stabilizes the singlet CT state, the observed dominance of this exchange mechanism serves as an explanation of why the CT state splittings have been found to be almost always negative and suggests that these results are not simulation artifacts.

Let us now consider the effects of allowing the CT state to undergo geometry relaxation. While crystal packing will generally reduce these effects by preventing full relaxation, the direction of the shift should be important. That is, if it is found that geometry relaxation stabilizes singlet CT states more than triplet CT states, it will support the previous conclusion that singlet CT states most often lie below triplet CT states. On the other hand, if geometry relaxation is found to destabilize the singlet CT state relative to the triplet CT state, it will suggest that, even if splittings obtained in the crystal structure geometry favor singlet CT states as in Table 2, the singlet CT state in the actual system may or may not be favored once partial relaxation has occurred.
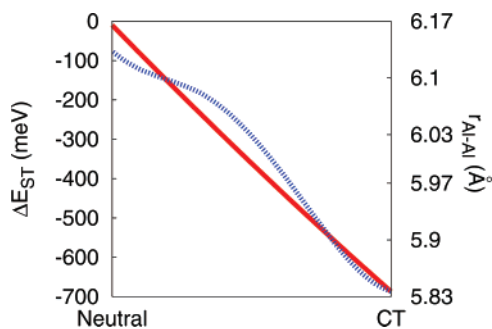
Figure 5. ΔE_{ST} (dotted line) and Al–Al distance (solid line) as a function of linear reaction coordinate connecting the crystal structure geometry (Neutral) with the optimized ⇅ CT state geometry (CT) for the α-Alq₃ dimer. We see that as geometry relaxation proceeds, the magnitude of ΔE_{ST} increases while the Al–Al distance decreases.

Table 3. Adiabatic ΔE_{ST} Values for Several CT State Heterodimers at the Relaxed ⇅ CT Geometry. Structural Relaxation Causes Substantial Stabilization of Singlets over Triplets

dimer	$\Delta E_{ST}(q_{ti})$ (meV)
Firpic⁻:DCM2⁺ [a]	−116
DCM⁻:CBP⁺ [b]	−329
α-Alq₃⁻:PtOEP⁺ [c]	−323

[a] Firpic = iridium(III)bis [(4,6-di-fluoropheny)-pyridinato-N,C²′]picolinate,[61] DCM2 = 4-dicyanomethylene-2-methyl-6-[2-(2,3,6,7-tetrahydro-1H,5H-benzo[ij]quinolizin-8-yl)vinyl]-4H-pyran.[62] [b] CBP = 4,4′-bis(9-carbazolyl)-2,2′-biphenyl[63] [c] PtOEP = 2,3,7,8,12,13,17,18-octaethyl-21H,23H-porphine platinum (II).[64]

To examine these issues, the optimal CT geometry was computed for Alq₃ beginning from the crystal structure for α-Alq₃ and relaxing the dimer in the mixed (⇅) CT state. The mixed state was chosen because it presents an idea of the "average" structures assumed by the singlet and triplet CT states. An approximate reaction coordinate was constructed by linear interpolation between the crystal structure geometry and the ⇅ CT state geometry, and ΔE_{ST} was computed as a function of this reaction coordinate, as shown in Figure 5. We observe that the singlet CT state lies below the triplet CT state along the entire coordinate and that the splitting increases monotonically as we proceed from the crystal structure to the CT structure. We can rationalize this singlet stabilization by noting that the Coulombic attraction present in the CT state causes the donor–acceptor distance to decrease as relaxation occurs (see Figure 5). This decreased distance results in increased orbital overlap, which causes an increase in kinetic exchange and thereby increases the singlet stabilization. We note that direct exchange should also increase in magnitude as the monomers approach one another, although apparently more slowly than the kinetic term. Additional evidence of this singlet stabilization trend was obtained by computing mixed-CT-state-optimized geometry splittings for three heterodimers (Table 3) selected because of their chemical relevance to the design of extrafluorescent OLEDs.[37] For each of these dimers, we again find that the splitting at the CT geometry strongly favors the singlet. We note that, while DFT tends to give unreliable structures for van der Waals complexes in general,[60] the relaxed CT geometries are dominated by charge–charge interactions between donor

and acceptor and as such should be well approximated by DFT. These results imply that, for systems in which singlet CT states are favored in the ground-state geometry, the singlet CT will be even more strongly favored as relaxation toward the CT state geometry occurs.

4. Discussion

Two experimental measurements of ΔE_{ST} for geminate electron–hole pairs in organic materials exist in the literature. Segal et al.[37] electrically excited an OLED containing Alq₃ and PtOEP to obtain $\Delta E_{ST} = -7$ meV. That is, they found the singlet CT state for that device to lie below the triplet CT state, in agreement with the energy ordering of the crystal structure and geometry-optimized splittings presented in Tables 2 and 3. On the other hand, Kadashchuk et al.[65] photoexcited poly-*p*-phenylene and measured its electroluminescence efficiencies as a function of temperature to find that the triplet CT state lies 3−6 meV below the singlet CT state, which has the opposite energy ordering of the majority of our calculations. However, since the magnitude and sign of the splitting has been found to be geometry-dependent (Figure 4), it is not unreasonable to suggest that the donor–acceptor structure studied by Kadashchuk may be the exceptional case where triplets are favored.

In either case, it is observed that the calculated splittings are typically an order of magnitude larger than the experimental splittings. Obviously, one concern is that this discrepancy arises from a systematic theoretical error. Most importantly, one notes that the CT states are diradicals, which are typically treated poorly in DFT because of nondynamic correlation.[66] While we cannot completely rule out these effects in the present case without significant computational expense (e.g., CASTPT2), we do note that constrained DFT is expected to reduce the influence of nondynamic correlation on the results.[39] In fact, simulations of the type presented here have been shown to have typical errors of only 10−20 meV for transition-metal exchange couplings,[39] so that the discrepancy in magnitude between theory and experiment is not expected to be due to the simulation method. Instead, it can be understood by recognizing that in a real device next-nearest and next-next-nearest neighbor CT states are generated along with their near-neighbor counterparts whereas the splittings calculated here correspond only to nearest-neighbor donor–acceptor pairs. To put it another way, the experiments probe an *ensemble* of structures of which we have considered only one representative. Since the magnitude of the splitting generally decreases with donor–acceptor pair orbital overlap and overlap decreases with pair distance, the splittings calculated here are expected to provide upper bounds for experimentally measured splittings. Thus, our results indirectly suggest that next-nearest and next-next-nearest neighbor CT states may play a significant role in these devices, a point that has not previously been appreciated. However, since we do not see a strong dependence of the *sign* of the splitting on distance (Table 2), our qualitative conclusions should remain valid even for non-nearest neighbors.

(60) Tsuzuki, S.; Lüthi, H. P. *J. Chem. Phys.* **2001**, *114*, 3949−3957.
(61) Tokito, S.; Iijima, T.; Suzuri, Y.; Kita, H.; Tsuzuki, T.; Sato, F. *Appl. Phys. Lett.* **2003**, *83*, 569−571.
(62) Hamada, Y.; Kanno, H.; Tsujioka, T.; Takahashi, H.; Usuki, T. *Appl. Phys. Lett.* **1999**, *75*, 1682−1684.
(63) Tao, Y. T.; Ko, C. W.; Balasubramaniam, E. *Thin Solid Films* **2002**, *417*, 61−66.
(64) Baldo, M. A.; O'Brien, D. F.; You, Y.; Shoustikov, A.; Sibley, S.; Thompson, M. E.; Forrest, S. R. *Nature* **1998**, *395*, 151−154.
(65) Kadashchuk, A.; Vakhnin, A.; Blonski, I.; Beljonne, D.; Shuai, Z.; Brédas, J. L.; Arkhipov, V. I.; Heremans, P.; Emelianova, E. V.; Bässler, H. *Phys. Rev. Lett.* **2004**, *93*, 066803.
(66) Dreuw, A.; Head-Gordon, M. *J. Am. Chem. Soc.* **2004**, *126*, 4007−4016.

The effects of the surrounding environment on CT state splittings have so far not been addressed, where the interactions to consider include steric, electrostatic, and van der Waals forces. In principle, the effects of steric interaction on the splitting could be studied by computing geometry-optimized splittings for systems containing nearest-neighbor and next-nearest-neighbor monomers. However, calculations on such large systems are generally computationally impractical, and as noted earlier, their effect would primarily be to reduce reorganization. However, since CT states contain a spatially separated electron and hole, they are expected to have large dipoles and to couple with polarizable groups in their vicinity. In other words, CT states are expected to have strong electrostatic interactions with their surroundings. We studied the effects of these interactions on the splitting in two ways. First, the dipoles of the singlet and triplet CT states were compared for each of the dimers in Table 2 where the difference in magnitudes between the singlet and triplet dipole moments is also shown. When this difference is small, the singlet and triplet state energies are expected to undergo similar relaxation in the presence of electrostatic interactions, thereby leaving ΔE_{ST} unaltered relative to the splitting obtained in vacuum. Note that the largest difference in dipole magnitude occurs for the $[Zn(tpy)_2]^{2+}$ homodimer, suggesting that it may be the most susceptible of these dimers to electrostatic interactions. To study this susceptibility more rigorously, the COSMO dielectric continuum model[67] with a dielectric constant of $\epsilon = 3$ was used to approximate the electrostatic effect on the donor–acceptor pair due to surrounding monomers. For the $[Zn(tpy)_2]^{2+}$ homodimer, the splitting with (without) the dielectric continuum was −73 meV (−85 meV). The similarity between the splittings obtained with and without a dielectric suggests that electrostatic interactions should not materially affect our conclusions even with modest differences between the singlet and triplet dipole magnitudes. This result is reasonable because ΔE_{ST} is a comparison of one CT state to another rather than a comparison of a CT state to the ground state, where dielectric effects would be expected to be larger. The final class of forces one might consider is van der Waals interactions. These forces are expected to be much weaker than either sterics or electrostatics, and thus, their effect on the splitting is not studied in detail here.

The simulations described so far allow mixing between the CT states, but do not consider the possibility that mixing might also occur between CT and high-lying exciton states. To put it another way, the constrained calculations assume that a full unit of charge has transferred from the donor to the acceptor, whereas one should expect a certain amount of leakage of the excess charge back on to the donor. Such mixing or leakage could increase charge recombination rates or induce intersystem crossing. To study this possibility, poly-*p*-phenylene was laterally displaced as in Figure 4 and energies for the CT and singlet exciton states were obtained using INDO/SCI[68,69] (Figure 6) and TDDFT[70] (Figure 7). We note that TDDFT by itself does not accurately predict the CT excitations in this system, placing

(67) Klamt, A.; Schüürmann, G. *J. Chem. Soc., Perkin Trans. 2* **1993**, *1993*, 799–805.
(68) Shuai, Z.; Brédas, J. L. *Phys. Rev. B: Condens. Matter Mater. Phys.* **1991**, *44*, 5962–5965.
(69) Cornil, J.; dos Santos, D. A.; Crispin, X.; Silbey, R.; Brédas, J. L. *J. Am. Chem. Soc.* **1998**, *120*, 1289–1299.
(70) Gross, E. K. U.; Dobson, J. F.; Petersilka, M. *Top. Curr. Chem.* **1996**, *181*, 81.
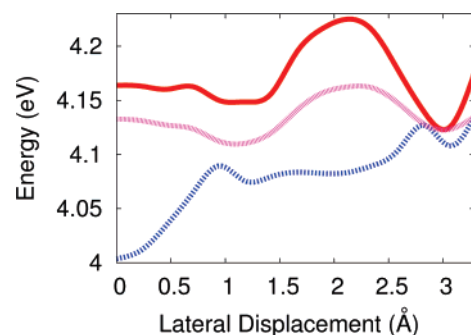
Figure 6. Excited state of poly-*p*-phenylene as a function of lateral displacement using INDO/SCI. In order of increasing energy, the states shown are second singlet exciton (dashed blue), triplet CT state (dotted magenta), and singlet CT state (solid red).
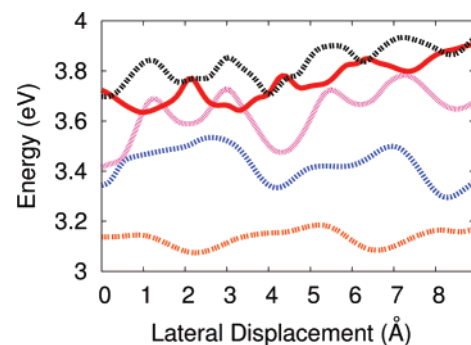

Figure 7. Excited state of poly-*p*-phenylene as a function of lateral displacement using TDDFT. In order of increasing energy, the states shown are the first singlet exciton (dashed orange), second singlet exciton (dashed blue), third singlet exciton (dotted magenta), singlet CT state (solid red), and triplet CT state (dashed black).

them more than 1 eV too low.[66] Hence, only the *intramolecular* excited states are described here with TDDFT, while the CT states are obtained from C-DFT, as before. Figure 6 shows avoided crossings of the CT and second exciton states at ≈1 and ≈3 Å using INDO/SCI. Thus, significant mixing is expected at these geometries. Meanwhile, if we compare the TDDFT exciton energies with the C-DFT CT state energies, we see that the curves cross at ≈1 and ≈3 (also ≈5 and ≈7) Å. As noted previously,[42] the DFT curves do not avoid one another because C-DFT states correspond to diabatic states which can undergo surface crossing. These four lateral displacements correspond to the four minima of ΔE_{ST} in the top figure of Figure 4. These results suggest that when the singlet CT state is most stabilized, nonluminescent exciton states can come quite close to the CT state and may play a significant role in the recombination process. We plan to investigate this process more fully in a later paper. For the present, we merely note that our results so far support the hypothesis that ΔE_{ST} plays a significant role in the recombination process but they do not disprove the possible further interference of dark excitons in the dynamics.[7]

Fluorescence efficiency within OLEDs is directly related to the fraction of singlet exciton states produced because only those states can fluoresce to emit light. This singlet state fraction can be increased above the statistically expected 25% if triplet CT states undergo rapid ISC to become singlet CT states. Meanwhile, given the extremely small (≈10^{-4} eV) spin–orbit coupling in organic molecules, favorable ISC typically requires that the CT states be very nearly degenerate. However, we have observed a nondegenerate CT state gap for the majority of

systems and geometries studied. These gaps are not so large that they could not in principle be overcome by unusually large spin−orbit or hyperfine interactions. However, typically the existence of a large gap suggests that a slower, activated process is required for intersystem crossing as compared with the traditional view of ISC arising from a purely degenerate mixing of spin states. Thus, in practice, it appears that the most effective means of enhancing the singlet fraction in OLEDs should be the incorporation of some transition-metal compound that is capable of increasing k_{ISC}. In fact, this principle has been verified in a recent OLED study[37] where predictions of ΔE_{ST} for the materials involved led to a clear interpretation of previously ambiguous results. The subsequent introduction of a sensitizing agent which selectively enhanced k_{ISC} resulted in an OLED with approximately 3-fold improvement in fluorescencing efficiency. Thus while the strong material dependence of ΔE_{ST} makes back-of-the-envelope predictions difficult, the ability to compute these splittings in an ab initio manner is still expected to assist in the development of more efficient OLEDs.

5. Conclusions

This Article outlines the results of some of the first high-level simulations of intermolecular electron−hole pair states in π-conjugated organic semiconducting materials. We find that the CT state singlet−triplet gap exhibits strong material dependence changing in magnitude and even sign depending on the character and relative orientation of the molecules involved. In agreement with ref 65, we find that in cofacial head-to-tail dimers the triplet CT state is favored. However, in nearly all other circumstances we find that singlet CT states are stabilized relative to triplet CT states for small dye molecules and oligomers and attribute this stabilization to kinetic exchange dominance. Structural relaxation is observed to cause additional stabilization of the singlet CT state, which is ascribed to the increased kinetic exchange that arises as donor approaches acceptor under the influence of Coulombic attraction. High-mobility semiconductors appear to give slightly larger ΔE_{ST} values, consistent with the idea that good electronic communication between donor and acceptor enhances kinetic exchange. Furthermore, the calculated magnitude of this gap, on the order of 50 meV for nearest neighbors, can be quite a bit larger than the average gap obtained in experiments, indicating the important role that next-nearest neighbors and other more distant pairs have on the experimental CT state gap.

These predictions have a direct impact on the design and understanding of OLEDs and the ultimate development of stable, high-efficiency blue and green fluorescent materials.[10,37] However, the chemistry discussed here applies just as well to any organic semiconductors composed of π-conjugated oligomers.

Thus, we would expect a similar interplay between singlet and triplet CT states in phthalocyanine dyes and derivitized bucky-balls that are often used in organic photovoltaics[71] and in pentacene films that are incorporated into organic transistors.[72] The open questions are how these ideas extend to polymeric systems, where both structural disorder and the formation of *intrachain* CT states will play significant roles in the kinetics, and inorganic/organic hybrid devices, where the delocalized nature of the inorganic carriers could lead to a picture of singlet and triplet states that involves itinerant, rather than localized, magnetism. Both of these directions are intensely interesting scientifically and will be the subject of future work.

Another central aim of future work is to find principles for controlling singlet−triplet CT state splittings in π-conjugated oligomeric materials. In particular, while not possible with available knowledge, a means for predictably modifying the donor−acceptor orbital overlap is desirable. For example, since ΔE_{ST} also has an important role in organic photovoltaics, where it is desirable for the triplet CT state to lie below the singlet CT state[71] so that recombination is *inhibited*, such control could also lead to more efficient and robust solar cells. In addition, a quantitative understanding of Marcus parameters for donor−acceptor pairs, including driving force, reorganization energy, and coupling, could also lead to greater control of OLED efficiency. The methodology for obtaining these parameters from C-DFT has been previously derived,[40,41] and the application of these techniques to organic materials such as those discussed here is actively being pursued. Rates of charge recombination could then be predicted in a first principles manner, for example, leading to a more thorough understanding of whether it is ΔE_{ST} or ΔG that causes the singlet/triplet ratio to deviate from 1:3.

Supporting Information Available: Dimer geometries used in calculations; complete ref 45. This material is available free of charge via the Internet at http://pubs.acs.org.

JA076125M

(71) Peumans, P.; Yakimov, A.; Forrest, S. R. *J. Appl. Phys.* **2003**, *93*, 3693−3723.
(72) Nelson, S. F.; Lin, Y. Y.; Gundlach, D. J.; Jackson, T. N. *Appl. Phys. Lett.* **1998**, *72*, 1854−1856.